Antibody-Fc/FcR interaction on macrophages as a mechanism for hyperprogressive disease in non-small cell lung cancer subsequent to PD-1/PD-L1 blockade

Antibody-Fc/FcR Interaction on Macrophages as a Mechanism for Hyperprogressive Disease in Non-Small Cell Lung Cancer Subsequent to PD-1/PD-L1 Blockade

Giuseppe Lo Russo[1]*, Massimo Moro[2]*, Michele Sommariva[3]*, Valeria Cancila[4]*, Mattia Boeri[2], Giovanni Centonze[2], Simona Ferro[5], Monica Ganzinelli[1], Patrizia Gasparini[2], Veronica Huber[5], Massimo Milione[6], Luca Porcu[7], Claudia Proto[1], Giancarlo Pruneri[6,8], Diego Signorelli[1], Sabina Sangaletti[9], Lucia Sfondrini[3], Chiara Storti[3], Elena Tassi[10,11], Alberto Bardelli[12,13], Silvia Marsoni[12,14], Valter Torri[7], Claudio Tripodo[4], Mario Paolo Colombo[9], Andrea Anichini[10], Licia Rivoltini[5], Andrea Balsari[3#], Gabriella Sozzi[2#§], Marina Chiara Garassino[1#]

[1]Thoracic Oncology Unit, Medical Oncology Department 1, Fondazione IRCCS - Istituto Nazionale dei Tumori, Milan (Italy)

[2]Tumor Genomics Unit, Department of Research, Fondazione IRCCS - Istituto Nazionale dei Tumori, Milan (Italy)

[3]Department of Biomedical Sciences for Health, University of Milan, Milan (Italy)

[4]Tumor Immunology Unit, Department of Health Sciences, Human Pathology Section, University of Palermo, Palermo (Italy)

[5]Immunotherapy of Human Tumors Unit, Department of Research, Fondazione IRCCS - Istituto Nazionale dei Tumori, Milan (Italy)

[6]Department of Pathology and Laboratory Medicine, Fondazione IRCCS - Istituto Nazionale dei Tumori, Milan (Italy)

[7]Computational Statistics Unit, Department of Oncology, IRCCS Istituto di Ricerche Farmacologiche Mario Negri, Milano (Italy)

[8] Dipartimento di Oncologia ed Emato-Oncologia, University of Milan, Milan (Italy)

[9]Molecular Immunology Unit, Department of Research, Fondazione IRCCS - Istituto Nazionale dei Tumori, Milan (Italy)

[10]Human Tumors Immunobiology Unit, Department of Research, Fondazione IRCCS - Istituto Nazionale dei Tumori, Milan (Italy)

[11]Experimental Hematology Unit, IRCCS San Raffaele Scientific Institute, Milano (Italy)

[12]Candiolo Cancer Institute-FPO, IRCCS, Candiolo (Italy)

[13] Department of Oncology, University of Torino, Candiolo (Italy);

[14]IFOM, Istituto Firc di Oncología Molecolare, Milan Italy

*These Authors contributed equally at this work

[#]These Authors contributed equally at this work as Senior Authors

[§] Corresponding author

Running title: ICI induce HP through FcR triggering on macrophages

Keywords: Hyperprogression; Non-small cell lung cancer; Immune checkpoint inhibitor; macrophages; Fc Receptor;

Financial support: This work was supported by Italian Ministry of Health (5 x 1000 Funds - 2014) (PI: Marina Chiara Garassino), by AIRC (Associazione Italiana per la Ricerca sul Cancro) (Grant Id:15190, PI: Andrea Balsari; Grant Id: 18812, PI: Gabriella Sozzi; Grant id:17431 PI:Andrea Anichini; Grant Id: 10137, PI: Mario P. Colombo), by EU project Horizon2020-686089 - PRECIOUS (PI: Licia Rivoltini), by Italian Ministry of Health (Grant Id: GR-2013-02355637, PI: Sabina Sangaletti). E. Tassi was supported by a fellowship from Fondazione Beretta-Berlucchi.

Corresponding Author:

Dr. Gabriella Sozzi

Tumor Genomics Unit, Department of Research,

Fondazione IRCCS - Istituto Nazionale dei Tumori,

Via Giacomo Venezian 1, 20133 Milan (Italy)

Tel. +390223902232; +393480199805

Fax. +390223902928

e-mail: gabriella.sozzi@istitutotumori.mi.it

Disclosure of Potential Conflicts of Interest

A.A. has received travel and accommodation expenses and institutional research funding from Bristol-Myers-Squibb; L.R. is being involved in scientific advisory boards, dissemination events and teaching programs for Bristol Meyer Squibb, Novartis, AstraZeneca, Merck and Pfizer; M.C.G is Advisory Board member of Bristol Meyer Squibb, MSD, Roche, Astra Zeneca, Novartis and Steering Committee member of MSD. All the other Authors declare no potential conflicts of interest.

Body text word count = 4131 words

Abstract word count = 249 words

Figures and tables = 5 (5 Figures, 0 Tables)

Supplementary Data: 5 (1 Supplementary Materials and Methods, 1 Supplementary Tables, 3 Supplementary Figures)

References = 31

ABSTRACT

Background: Hyperprogression (HP), a paradoxical boost in tumor growth, was described in a subset of patients treated with immune checkpoint inhibitors (ICI). Neither clinico-pathological features nor biological mechanisms associated with HP have been identified.

Methods: Among 187 patients with non-small cell lung cancer (NSCLC) treated with ICI at our Institute, cases with HP were identified according to clinical and radiological criteria. Baseline histological samples from patients treated with ICI were evaluated by immunohistochemistry (IHC) for myeloid and lymphoid markers. T-cell deficient mice, injected with human lung cancer cells and patient-derived xenografts (PDXs) belonging to specific mutational subsets, were assessed for tumor growth after treatment with antibodies against mouse and human programmed death receptor-1 (PD-1). The immune microenvironment was evaluated by flow cytometry and IHC.

Results: Among 187 patients, 152 were evaluable for clinical response. We identified 4 categories: 32 cases were defined as Responders (21%), 42 patients with Stable Disease (27.7%), 39 cases defined as Progressors (25.7%) and 39 patients with HP (25.7%). Pre-treatment tissue samples from all patients with HP showed tumor-infiltration by M2-like $CD163^{+}CD33^{+}PD\text{-}L1^{+}$ clustered epithelioid macrophages. Enrichment by tumor-associated macrophages (TAM) was observed, even in tumor nodules from immunodeficient mice injected with human lung cancer cells and with PDXs. In these models, tumor growth was enhanced by treatment with anti-PD-1, but not by anti-PD-1 $F(ab)_2$-fragments.

Conclusions: These results suggest a crucial role of TAM reprogramming, upon Fc receptor engagement by ICI, eventually inducing HP and provide clues on a distinctive immunophenotype potentially able to predict HP.

STATEMENT OF TRANSLATIONAL RELEVANCE

Hyperprogressive disease in lung cancer and other tumors is an urgent clinical issue reaching 1 out of 5 patients treated with ICI, affecting their prognosis and leading to death in a very short time. As the use of immunotherapy increases in the clinic, it is important to understand the intricacies of this new treatment option in order to optimize treatment approaches. Data already published in the field mainly focused on adaptive immunity without finding any characteristics to predict a priori the phenomenon. Our preclinical findings underline the role of innate immunity in mediating hyperprogression via Fc/FcR triggering on macrophages by anti-PD1 antibody. Accordingly, all patients with HP showed tumor-infiltration by M2-like $CD163^{+}CD33^{+}PD\text{-}L1^{+}$ clustered epithelioid macrophages. These results, pointing to the involvement of innate immune cells in HP, provide new insights into the still unknown mechanisms behind a clinical conundrum.

INTRODUCTION

The advent of immune checkpoint inhibitors (ICI) has radically changed the paradigm of care for patients with non-small cell lung cancer (NSCLC). Several agents are now approved in the treatment of NSCLC based on their superiority over chemotherapy (1,2). Immunotherapy with antibodies targeting either the programmed death receptor 1 (PD-1) or its ligand (PD-L1) may provide long-term benefits in approximately 20% of patients (2). However, in a subset of patients, ICI paradoxically accelerates tumor growth, a phenomenon known as hyperprogression (HP) (3–6). Studies have estimated that the prevalence of HP in patients with different cancer histotypes treated with ICI may range between 9% and 29% (3–6). No significant histopathological and molecular features capable of predicting *a priori* HP have been identified, with the partial exception of rare *MDM2* amplification and epidermal growth factor receptor (*EGFR*) mutations (5). These observations have ignited an international debate regarding whether HP is a true phenomenon or only representative of a subset of patients with a particularly worse prognosis.

In the tumor microenvironment, the effector functions of innate immune cells may be blunted by the PD-1 receptor, as observed for T lymphocytes, suggesting that these innate cells are another potential target for ICI (7–9). Accordingly, it has been demonstrated that anti-PD-1 antibody can exert antitumor activity in immunodeficient mice via natural killer (NK) cells (8). Conversely, it has been demonstrated that, in PD-1$^{-/-}$ NK cells or in NK cells pre-treated with anti-PD-1 antibody, the production of lytic molecules such as perforins and granzymes is decreased (10). Moreover, tumor-infiltrating dendritic cells (9) and monocytes (11) are reported to release the immunosuppressive cytokine interleukin-10 upon anti-PD-1 treatment. Therefore, it is possible to hypothesize that in some circumstances, PD-1 blockade might exacerbate immunosuppression upon interaction with innate immune cells.

The aim of this study was to investigate, at the clinical and pathological level, the phenomenon of HP in NSCLC patients and to evaluate the role of innate immunity during ICI treatment. To

133 eliminate the interference of T lymphocytes we exploited cell lines and patient derived xenografts
134 (PDXs) transplanted in immunodeficient mice.
135

MATERIAL AND METHODS

Clinical Series

Medical records, radiological findings, and available tumor specimens were collected from patients with NSCLC treated with ICI at the Thoracic Unit of the Istituto Nazionale dei Tumori, Milan, Italy, from July 2013 to December 2017.The study complied with the Declaration of Helsinki and was done in accordance with good clinical practice guidelines. All samples were obtained according to the Internal Review and the Ethics Boards of the Istituto Nazionale Tumori of Milan and all patients provided informed consent. All experimental protocols were approved by the Ethics Boards of the Istituto Nazionale Tumori of Milan (Int 22/15). Radiological evaluation (computed tomography scan with or without brain magnetic resonance imaging) was performed at treatment initiation and every 8 weeks thereafter. Considering that criteria to define patients with HP described by previous authors (3-6) are applicable only in advanced lines, our multidisciplinary team (oncologists, pneumologists, radiologists, and thoracic surgeons) created institutional clinical and radiological criteria designed to identify patients with HP also in first line treatment. Patients with HP or those patients defined as P were classified according to predefined criteria as follows: i) Time-to-treatment failure < 2 months (Time to treatment failure is defined as the time from the start of treatment with ICI to ICI discontinuation for any reason, including progression, patient preference, toxicity or death); ii) Increase of ≥ 50% in the sum of target lesions major diameters between baseline and first radiological evaluation; iii) Appearance of at least two new lesions in an organ already involved between baseline and first radiological evaluation; iv) Spread of the disease to a new organ between baseline and first radiological evaluation; v) Clinical deterioration with decrease in ECOG performance status ≥ 2 during the first 2 months of treatment.

Patients who fulfilled at least three of the clinical/radiological criteria were defined as exhibiting HP, while patients with RECIST 1.1 progressive disease as best response without fulfilling at least three criteria were defined as P patients. All R patients and SD patients were classified according to

their RECIST 1.1 best response. Only patients who underwent at least two cycles of ICI treatment were included in the present analysis.

Immunohistochemistry

Immunohistochemistry was carried out on Formal-fixed Paraffin embedded human or PDX tissue sections as described in Supplementary materials and methods. All the slides were analyzed under a Zeiss Axioscope-A1 equipped with fluorescence module and microphotographs were collected using a Zeiss Axiocam 503 Color with the Zen 2.0 Software (Zeiss, Oberkochen DE). All markers were scored according to the percentage of immunoreactive cells out of the total cellularity.

Animals Studies

All xenograft experiments were undertaken using 8- to 9-week-old female athymic nude or SCID mice (Charles River Laboratories, Calco, Italy). Human NSCLC cell line H460 tumor-bearing athymic nude mice were treated i.p. or peri-tumorally (p.t.) with either 200 µg of monoclonal antibody anti-mouse PD-1 (clone RMP1-14, BioXCell) or saline, and with either p.t. anti-PD-1 $F(ab)_2$ or isotype control. Experiments were carried out in groups of four SCID mice, bearing a PDX sample or a cell suspension (10^5 cells for H460 and PC9 xenograft experiments) in each flank. Mice were treated twice weekly with an i.p. injection of 10 mg/kg Nivolumab (Opdivo, Bristol-Myers Squibb) or Nivolumab $F(ab)_2$ fragments. Mice were maintained in the Animal Facility of the Fondazione IRCCS Istituto Nazionale dei Tumori. Animal experiments were authorized by the Institutional Animal Welfare Body and the Italian Ministry of Health, and performed in accordance with National law (D.lgs 26/2014) and Guidelines for the Welfare of Animals in Experimental Neoplasia (12). At the end of each experiment, tumors were harvested for subsequent analyses.

Statistical Analysis

Distribution of continuous and categorical biomarkers was summarized by the median as a measure of central tendency and absolute frequencies, respectively. The Cochran–Mantel–Haenszel chi-square test was used to detect statistical association (i.e. $P < 0.05$) in univariate analysis. The median and interquartile range (IQR), follow up was estimated using the reverse Kaplan-Meier method.

RESULTS

Clinical and Pathological Evidence in Patients with Advanced NSCLC Treated with ICI

From July 2013 to December 2017, 187 patients with advanced NSCLC received treatment with ICI at the Thoracic Unit of the Medical Oncology Department at the Istituto Nazionale dei Tumori, Milan, Italy, and 152 patients were evaluable for response. We identified 4 categories: Responders (R, 32 cases, 21%), patients with Stable Disease (SD, 42 cases, 27.7%), Progressors (P, 39 cases,25.7%), and patients with HP (39 cases, 25.7%). Patients' characteristics are described in Supplementary Table S1. In this population, after a median follow-up of 32.7 (IQR 15.1-39.6) months, 108 out of 152 patients (71%) died. Median (95% CI) Overall Survival (OS) in the overall population was 11.9 (95% CI 8.8-15.5) months.

If we restrict the analysis to patients with HP, median OS significantly decreased to 4.4 (95% CI 3.4-5.4) months as compared to 17.7 (95%CI 13.4 -24.1) in non HP patients. Median OS was 8.7 (95% CI 5.3-13.4), 17.7 (95% CI 12.7-25.5) and not reached in P, SD and R patients, respectively.

Supplementary Table S2 shows the differences between P and HP according to our criteria described in the Materials and Methods section. Of 187 patients, 64 were diagnosed in other centers and could not be included in the present histopathological and molecular analysis. Of the remaining 123, 35 patients (11 with HP and 24 without HP) were evaluable for response and had tissue samples suitable for a wide immunohistochemical characterization and gene expression analysis. Patients' characteristics of the extensively analyzed 35 samples resembles the clinical characteristics of the whole treated population

Immunohistochemical analysis was performed to assess the presence and distribution of tumor-infiltrating immune elements. The immunophenotype of 11 patients with HP was compared to that of 24 patients without HP (6 P, 11 SD and 7 R). No significant differences were observed among all the clinical classes of patient with respect to the subsets of tumor-infiltrating T lymphocytes (TILs), evaluated by the density of $CD3^+$, $CD4^+$, and $CD8^+$ lymphocytes and $FOXP3^+$ regulatory T cells (Tregs). In addition, no differences were detected between classes of patient in the numbers of

CD138$^+$ plasma cells (PCs), CD123$^+$ plasmacytoid dendritic cells (pDCs), peritumoral and stromal myeloperoxidase (MPO)$^+$ myeloid cells, CD163$^+$ macrophages, CD33$^+$, PD-1 and PD-L1$^+$ immune cells. However, MPO$^+$ myeloid cells within the tumor were directly correlated (P= 0.0497) and PD-L1 expression in tumor cells was inversely correlated (P= 0.0457) with HP. Furthermore, a statistical trend was shown for the M2 macrophage/myeloid derived suppressor cells marker, Arginase-A I (ArgI) on peritumoral immune cells (P =0.0666) (Supplementary Table S3).

Gene expression profile (GEP) analysis of pre-treatment tumors did not show any relevant features except for under-expression of pathways related to proliferative activity and cell metabolism in patients experiencing HP after ICI (Supplementary Figures S1A and S1B). The analyses of selected genes representative of immune subsets by RT-qPCR revealed overexpression of the *CD274* gene, encoding for PD-L1, as the only significant marker in R patients (Supplementary Figure S1C). Fluorescence in situ hybridization of *MDM2* and *MDM4* genes, carried out on in a cohort of 30 FFPE NSCLC tissue derived from 11 patients with HP and 17 patients without HP, revealed the presence of 3 amplified tumors (2 *MDM2*, 1 *MDM4*) in patients with HP and 6 amplified tumors (4 *MDM2*, 1 *MDM4* and 1 *MDM2* and *MDM4*) in patients without HP (Supplementary Figure S2).

Notably, we noticed that, in some cases, CD163$^+$ tumor-infiltrating macrophages showed epithelioid morphology (alveolar macrophage-like) with the tendency to form dense clusters within neoplastic foci (Figure 1A). In these cases, the same cells were found to co-express CD33 and PD-L1 (Figure 1B and Figure 2). Such a peculiar morphology, aggregation, and immunophenotype (CD163$^+$CD33$^+$PD-L1$^+$) of macrophages, which we define "complete immunophenotype", was observed in all patients with HP and found to be statistically significant versus patients without HP (P<0.0001) (Supplementary Tables S4 and S5). This complete immunophenotype was also observed in one P patient, two patients with SD, and one R patient (Supplementary Table S5). All other cases experiencing treatment response with stable or slowly progressive disease either lacked the presence of epithelioid macrophages or showed loose clustering, or lacked some of the above markers (mainly CD33$^-$ and/or PD-L1) (Figure 1C and 1D).

Anti Mouse PD-1 Antibody Induces Tumor Progression in Athymic Mice

Histopathological analyses showed the presence of clustered $CD163^{+}CD33^{+}PD\text{-}L1^{+}$ epithelioid macrophages as a distinctive trait in tumors with HP. Therefore, we sought to test whether macrophages are involved in the detrimental effects associated with anti-PD-1 therapy in preclinical models. Athymic nude mice implanted with human H460 NSCLC cell line were treated either intraperitoneally (i.p.) (Figure 3A) or peritumorally (p.t.) (Figure 3B) with anti-PD-1 antibody (clone RMP1-14) or saline. Anti-PD-1 treatment increased tumor growth compared with the control group, regardless of route and schedule of treatment (Figure 3A and 3B). Anti-PD-1 treatment was also associated with a significant increase in $CD45^{+}$ leukocyte infiltration at the host–tumor interface, evaluated by immunohistochemistry (IHC) (Figure 3C). Such an increase was mainly due to increasing numbers of intratumoral macrophages ($F4/80^{+}$ cells) and Arginase-I^{+}-expressing cells, whereas the density of B lymphocytes ($CD45R/B220^{+}$), granulocytes ($Gr\text{-}1^{+}$) and NK ($NKp46^{+}$) cells was comparable to the control group (Figure 3C). Of note, Arginase-I was also consistently expressed by the complete immunophenotype intra-tumor macrophages characterizing patients with HP (Figure 1E). Tumor-associated macrophages (TAMs) can express PD-1 and the blocking of this receptor restores antitumor functions (7). Thus, the detrimental boost in tumor growth may not be ascribed to such receptor blockade, but rather to the Fc domain of the antibody which is reported to modulate anti-PD-1 antibody functional activity (13). Accordingly, the same experiments were performed using anti-PD-1 $F(ab)_2$ fragments. The lack of the Fc portion abrogated the increase in tumor growth observed with the whole antibody (Figure 3D).

Anti Human PD-1 Antibody (Nivolumab) Induces Tumor Progression of PDXs in SCID Mice

To exclude a direct involvement of PD-1 expression in immune cells, we treated severe combined immunodeficient (SCID) mice with anti-human PD-1 (Nivolumab) which does not cross-react with the murine counterpart (Supplementary Figure S3A). Since a link between HP and *EGFR* mutational status has been proposed by Kato et al. (5), we compared two NSCLC PDXs, with and without *EGFR* mutation: PDX302 ($P53^{C135Y}$, $EGFR^{L858R}$, $KRAS^{WT}$, APC^{WT}) versus PDX305

(P53^{WT}, EGFR^{WT}, KRAS^{G12C}, APC^{R1114L}). On PDXs, before treatment, fluorescence-activated cell sorting (FACS) analysis with human anti-PD1 antibody showed expression of PD-1 receptor on a subset of tumor cells (around 1% PD-1^{+} cells, Supplementary Figure S3B). In addition, IHC analysis showed that F4/80^{+} epithelioid/monocytoid elements, aggregated in clusters resembling those identified in patients with HP, were appreciable only in PDX302 (Supplementary Figure S3C).

SCID mice carrying subcutaneous PDX302 (n = 8), but not PDX305 (n = 8), showed a significant increase in tumor growth rate compared with controls following twice weekly treatment with Nivolumab (Figure 4A). FACS analysis in lungs of PDX302 bearers showed increased cancer cell dissemination in Nivolumab-treated mice but not in controls (3.88±1.99% vs. 0.87±0.33%, P = 0.0286, respectively) (Figure 4B), whereas no differences were detected in PDX305 bearers (data not shown).

FACS analysis was also performed on primary tumors for characterization of different myeloid subsets (CD11b, Ly6G, Ly6C, F4/80) and NK cells (CD49b). In PDX302-bearing mice, an increase in CD11b^{+}F4/80^{high} macrophages was observed in the Nivolumab-treated group versus controls (Supplementary Figure S3D), whereas no significant changes occurred in other immune subpopulations. Accordingly, IHC analysis performed on the same tumors revealed accumulation of macrophages and ArgI^{+}-expressing cells (Figure 4C and Supplementary Figure S3E). Notably, in PDX302 the F4/80^{+} epithelioid/monocytoid clusters were enriched in Nivolumab-treated tumors (Figure 4C).

Overall, these data indicate that, in the *EGFR*-mutated PDX302-bearing mice, Nivolumab triggers a detrimental effect characterized by increased tumor growth, lung dissemination and the accrual of macrophages, most likely M2.

To further confirm the detrimental effect induced by Nivolumab in other preclinical models, PDX111 (P53^{C242X}, KRAS^{G12V}, CDKN2A ^{E69X}, CTNNB1^{T41I}), PDX220 (wild type for all tested genes), H460 (KRAS^{Q61H}, STK11^{Q37*}), and PC9 (EGFR^{L858R}, EGFR^{E746_A750del}, CDKN2A^{G67V}) were

296 xenografted in SCID mice. All tested models showed low levels of PD1-expression on tumor cells
297 (ranging from 0.6 to 4%, Supplementary Figure S3B). As with PDX302, an increase in tumor
298 growth was observed in H460- and PC9-bearing mice after Nivolumab treatment. PDX111 tumors
299 showed a variable response, whereas tumors in PDX220- and PDX305-bearing mice showed no
300 response to Nivolumab (Figure 4D).
301 To reinforce the role of the Fc domain of the antibody in boosting tumor growth, PDX302-bearing
302 SCID mice were treated with Nivolumab-F(ab)$_2$ fragments. No HP-like growth was observed
303 (Figure 4E) whereas in the same experiment mice treated with the entire antibody showed HP-like
304 growth, dissemination to lung (Figure 4F) and regional (iliac) lymph node metastases (Figure 3G).
305 In the group pretreated with clodronate, which reduces F4/80$^+$ macrophages, impaired Nivolumab-
306 induced tumor growth was observed (Figure 4E). The F4/80$^+$ macrophages also stained for CD206
307 that marks M2-like subsets and aggregated in fibrotic-like areas in Nivolumab- but not in
308 Nivolumab F(ab)$_2$-treated tumors. In the latter less fibrotic areas than in control mice were observed
309 (Figure 4H).
310 These results suggest that HP is sustained by Nivolumab interaction with M2-like macrophages,
311 most likely via Fc-Fcγ receptor binding (Figure 5).
312

DISCUSSION

Although ICI have changed the paradigm of care for patients with NSCLC, an in-depth examination of the Kaplan-Meier curves from the CheckMate-026 (14), CheckMate-057 (15), CheckMate-227 (16), and KEYNOTE-042 (17) trials showed an excess of disease progression and death in the immunotherapy treatment arms compared with chemotherapy in the first 3 months of treatment. This was also underscored by the European Medicines Agency in response to the appraisal for the second-line use of Nivolumab in non-squamous histologies (http://www.ema.europa.eu/docs/en_GB/document_library/EPAR_-_Product_Information/human/003985/WC500189765.pdf). Furthermore, the benefit of ICI in trials conducted in never smokers and in patients with *EGFR* mutation-positive or Anaplastic Lymphoma Kinase (*ALK*)-mutation-positive NSCLC seems unclear (1,2,5,14,15). The four most important papers on the HP topic showed prevalence rates ranging from 9% to 29% throughout tumor types, including NSCLC (3–6). In all these papers, the ratio of the tumor growth rates before and during ICI treatment was used to identify HP, although with slightly different cut-offs. None of these studies defined pathological features able to predict HP, although *MDM2/4* amplification and *EGFR* alterations were proposed to be associated (5). However, we did not find any significant difference in the frequency of *MDM2/4* amplification between patients with and without HP, and the role of *EGFR* cannot be discussed due to the low number of *EGFR*-mutated patients included in our case series (Supplementary Table S1)

Our definition of HP is different from that used in the above-mentioned studies, where radiological imaging before, at the start and after ICI is needed to identify HP. However, in clinical practice all these radiological evaluations are often unavailable, and as a consequence, the criteria used in literature are unable to classify patients with HP considering that ICI are starting to be widely used as first line therapy. Furthermore, both Response Evaluation Criteria In Solid Tumors (RECIST) 1.1 and Immune-related Response Evaluation Criteria In Solid Tumors (irRECIST) criteria, used in the

reported analyses, considered only changes in tumor size and did not take into account non-target lesions, such as lymphangitis and pathological lesions under 10 mm. In addition, functional and clinical aspects, such as deterioration in performance status, were not considered. Therefore, we decided to include both clinical and radiological criteria to identify patients with HP in our series. These proposed criteria might overestimate the real fraction of patients experiencing HP; for these reasons, a clinical trial is ongoing within our Institute to properly validate the criteria and thereby obtain the true rate of HP as well as the distinctive immunophenotype.

Nivolumab-treated cell lines and PDX-bearing SCID mice mirrored the clinical observation of HP following treatment with ICI. Interestingly, patients and mice classified with HP share a similar tumor immunophenotype. Indeed, the population of $F4/80^{+}CD206^{+}Arginase\text{-}A1^{+}$ cells emerging from PDXs with HP matches macrophage features of the human counterpart (Figures 1A, 4C, 4H and Supplementary Figure S3C). M2-like macrophages were preferentially associated with fibrotic foci in PDXs that experience HP-like tumor growth after PD-1 blockade. The recruitment of these myeloid cells may promote a peculiar cancer-associated innate response that may affect tumor growth. Indeed, Knipper at al. described a cross-talk between myeloid cells and fibroblasts promoting skin fibrosis that could provide proliferative and pro-survival signals in cancer cells (18). Prominent mitotic figures can be consistently identified in Nivolumab-treated tumor foci embedded in a fibrotic stroma. In human samples, the accumulation of these cells is apparently unrelated to the extent and distribution of tumor-infiltrating T-cell populations.

The role of the innate immune system in mediating the effects of ICI is now clearly emerging. Cells of myeloid origin present in the tumor microenvironment decrease the effects of ICI via PD-L1 expression (19), by “stealing” anti-PD-1 antibody from the membrane of T lymphocytes that return to anergy (20) or by secreting immunosuppressive molecules (21). Our study provides novel evidence of negative immuno-regulatory role exerted by $PD\text{-}L1^{+}$ macrophages enriched at tumor site under treatment with ICI. Pre-treatment lesions from all patients classified as HP showed tumor infiltration by clustered epithelioid macrophages characterized by a $CD163^{+}CD33^{+}PD\text{-}L1^{+}$ profile.

Interestingly, $CD163^+$ $PD\text{-}L1^+$ macrophages represent a common immune landscape for different tumors. $PD\text{-}L1^+$ macrophages have been recently described to accumulate in tight clusters at the tumor invasive margin in NSCLC (22). Macrophages expressing both PD-L1 and the "M2" marker CD163 have been described in MSI-colorectal cancer (23), triple-negative breast cancer (24), gastric and cervical cancer (25,26). In some of these studies, the presence of $PD\text{-}L1^+$ macrophages has been associated with poor prognosis (24,26) and/or with immunosuppressive function through IL-10 production (27). In addition, the concurrent expression of CD163, CD33, and PD-L1 has been recently described in alveolar macrophages from acute respiratory distress syndrome patients, a non oncological condition present in 10% of subjects admitted to intensive care units (28). In this regard, we observed an increased infiltration of M2 macrophages after anti-PD-1 administration, providing evidence for their involvement in determining HP. TAMs can also express PD-1 that, if neutralized, can restore M1-like properties (7). This likely excludes blockade of PD-1 signaling in our models that remain rather oriented to M2. Therefore, we examined the possibility of FcR engagement as a modulator of anti-PD-1 activities (13). Upon testing the $F(ab)_2$ moiety in comparison to whole Ab, we have shown that Nivolumab without the Fc domain no longer induces HP-like disease in our models.

The anti-mouse PD-1 clone RMP1-14, utilized for the treatment of tumor-bearing athymic mice, is a rat immunoglobulin IgG2a reported to interact with the mouse inhibitory receptor, FcγRIIb (13). FcγRIIb has been shown to be involved in dampening the immune response, and impairments in FcγRIIb function are associated with an exacerbation of inflammatory processes (29). The anti-human PD-1 antibody Nivolumab is an IgG4 isotype with reduced binding affinity to activating FcγRs, thereby avoiding antibody-dependent cell-mediated cytotoxicity on $PD\text{-}1^+$ immune cells (30). However, Nivolumab maintains the ability to bind to the inhibitory FcγRIIb receptor (13). Therefore, we suggest a possible role of FcγRIIb in the detrimental effect associated with anti-PD-1 therapy. However, since both human IgG4 and rat IgG2a can bind at lower affinity to other FcRs, the involvement of these receptors cannot be excluded. Further studies elucidating the involvement

of FcRs in the development of HP are required. Very recently, a report described PD-1 expression in one NSCLC case with HP and in one mouse NSCLC cell line. The latter treated with anti murine PD-1 Ab underwent accelerated tumor growth (31). This interesting and logical explanation of HP can't be totally supported by the low expression/prevalence of PD-1 on tumors and by $F(ab)_2$ experiments in mice. We found clusters of PD-1 expressing cells in 2 out of 11 patients with HP (data not shown) and in all xenografts and PDXs, although at low levels (0.6 - 4%) and with no correlation with HP-like progression.

In conclusion, the ongoing debate regarding whether HP is a true phenomenon or only representative of patients with a particularly worse prognosis is confirmed in our preclinical models, where ICI are able to boost tumor growth in a manner akin to the clinical observations of HP in patients with NSCLC. Our results suggest that FcR triggering of clustered epithelioid macrophages with a specific immunophenotype by ICI delivers a signaling cascade that promotes functional reprogramming of these cells toward a more aggressive pro-tumorigenic behavior. This eventually induces HP in a subset of patients with distinctive immune and genetic profiles (depicted in Figure **5**). Our analyses, for the first time, suggest a role of innate immunity in this process. A further prospective validation of the HP immunophenotype and its relationship with specific genotypes, as well as the new proposed clinical criteria to classify HP, is ongoing.

Authors' Contributions

Conception and design: GS, MCG , ABardelli, SM, LR, AA, ABalsari

Development of methodology: VC, GC, SF, PG, CS

Acquisition of data: CT, MMilione, MB, MS, MMoro, GL, PG, MG, VH, CP, DS, ET, SS

Analysis and interpretation of data: CT, MMoro, MS, GL, GP, LP, VT, CP, DS, LS, SS

Writing, review and/or revision of the manuscript: ABardelli, SM, MS, MMoro, MG CP, DS, GL, MPC, CT, GA, AA, ABalsari, LR, GS, MCG

Study supervision: MPC, GS, MCG, GA

Acknowledgments

The authors wish to thank the following individuals: Dr M. Figini for the production of Nivolumab-F(ab)$_2$; Dr L. De Cecco for GEP profiles; Dr M. Dugo for bioinformatic analyses; Mrs A. Cova and Dr A. Berzi for technical assistance; Dr A. Martinetti for biological sample collection; Dr E. Tagliabue for data discussion and interpretation; Dr G. Morello for her precious support in performing double-marker immunolocalization analyses, and Dr G. Apolone for continuous support in the planning and execution of the study and for scientific writing. The authors would also like to acknowledge the editorial assistance provided by Chris Cammack, a professional medical writer at Ashfield Healthcare Communications, an Ashfield Company, part of UDG Healthcare plc (Tytherington, UK).

REFERENCES

1. Califano R, Kerr K, Morgan RD, Lo Russo G, Garassino M, Morgillo F, et al. Immune Checkpoint Blockade: A New Era for Non-Small Cell Lung Cancer. Curr Oncol Rep. Current Oncology Reports; 2016;18.
2. Assi HI, Kamphorst AO, Moukalled NM, Ramalingam SS. Immune checkpoint inhibitors in advanced non–small cell lung cancer. Cancer. 2018;124:248–61.
3. Champiat S, Dercle L, Ammari S, Massard C, Hollebecque A, Postel-Vinay S, et al. Hyperprogressive disease is a new pattern of progression in cancer patients treated by anti-PD-1/PD-L1. Clin Cancer Res. 2017;23:1920–8.
4. Saâda-Bouzid E, Defaucheux C, Karabajakian A, Coloma VP, Servois V, Paoletti X, et al. Hyperprogression during anti-PD-1/PD-L1 therapy in patients with recurrent and/or metastatic head and neck squamous cell carcinoma. Ann Oncol Off J Eur Soc Med Oncol. 2017;28:1605–11.
5. Kato S, Goodman A, Walavalkar V, Barkauskas DA, Sharabi A, Kurzrock R. Hyperprogressors after immunotherapy: Analysis of genomic alterations associated with accelerated growth rate. Clin Cancer Res. 2017;23:4242–50.
6. Ferrara R, Caramella C, Texier M, Valette CA, Tessonnier L, Mezquita L, et al. Hyperprogressive disease (HPD) is frequent in non-small cell lung cancer (NSCLC) patients (pts) treated with anti PD1/PD-L1 monoclonal antibodies (IO). Ann Oncol. Oxford University Press; 2017;28:abstract 1306PD.
7. Gordon SR, Maute RL, Dulken BW, Hutter G, George BM, McCracken MN, et al. PD-1 expression by tumour-associated macrophages inhibits phagocytosis and tumour immunity. Nature. Nature Publishing Group; 2017;545:495–9.
8. Liu Y, Cheng Y, Xu Y, Wang Z, Du X, Li C, et al. Increased expression of programmed cell death protein 1 on NK cells inhibits NK-cell-mediated anti-tumor function and indicates poor prognosis in digestive cancers. Oncogene. 2017;36:6143–53.

9. Lamichhane P, Karyampudi L, Shreeder B, Krempski J, Bahr D, Daum J, et al. IL10 release upon PD-1 blockade sustains immunosuppression in ovarian cancer. Cancer Res. 2017;77:6667–78.

10. Solaymani-Mohammadi S, Lakhdari O, Minev I, Shenouda S, Frey BF, Billeskov R, et al. Lack of the programmed death-1 receptor renders host susceptible to enteric microbial infection through impairing the production of the mucosal natural killer cell effector molecules. J Leukoc Biol [Internet]. 2015;99:2–9.

11. Said EA, Dupuy FP, Trautmann L, Zhang Y, Shi Y, El-Far M, et al. Programmed death-1-induced interleukin-10 production by monocytes impairs CD4 + T cell activation during HIV infection. Nat Med [Internet]. Nature Publishing Group; 2010;16:452–9.

12. Workman P, Aboagye EO, Balkwill F, Balmain A, Bruder G, Chaplin DJ, et al. Guidelines for the welfare and use of animals in cancer research. Br J Cancer. 2010;102:1555–77.12

13. Dahan R, Sega E, Engelhardt J, Selby M, Korman AJ, Ravetch J V. FcγRs Modulate the Anti-tumor Activity of Antibodies Targeting the PD-1/PD-L1 Axis. Cancer Cell. Elsevier; 2015;28:285–95.

14. Carbone DP, Reck M, Paz-Ares L, Creelan B, Horn L, Steins M, et al. First-Line Nivolumab in Stage IV or Recurrent Non–Small-Cell Lung Cancer. N Engl J Med. 2017;376:2415–26.

15. Borghaei H, Paz-Ares L, Horn L, Spigel DR, Steins M, Ready NE, et al. Nivolumab versus Docetaxel in Advanced Nonsquamous Non–Small-Cell Lung Cancer. N Engl J Med. 2015;373:1627–39.

16. Hellmann MD, Ciuleanu T-E, Pluzanski A, Lee JS, Otterson GA, Audigier-Valette C, et al. Nivolumab plus Ipilimumab in Lung Cancer with a High Tumor Mutational Burden. N Engl J Med [Internet]. 2018;NEJMoa1801946.

17. Lopes G, Wu Y-L, Kudaba I, Kowalski D, Chul Cho B, Castro G, et al. Pembrolizumab (pembro) versus platinum-based chemotherapy (chemo) as first-line therapy for advanced/metastatic NSCLC with a PD-L1 tumor proportion score (TPS) ≥ 1%: Open-label,

phase 3 KEYNOTE-042 study. J Clin Oncol. 2018;36:suppl. abstr. LBA4.

18. Knipper JA, Willenborg S, Brinckmann J, Bloch W, Maaß T, Wagener R, et al. Interleukin-4 Receptor α Signaling in Myeloid Cells Controls Collagen Fibril Assembly in Skin Repair. Immunity. 2015;43:803–16.

19. Antonios JP, Soto H, Everson RG, Moughon D, Orpilla JR, Shin NP, et al. Immunosuppressive tumor-infltrating myeloid cells mediate adaptive immune resistance via a PD-1/PD-L1 mechanism in glioblastoma. Neuro Oncol. 2017;19:796–807.

20. Arlauckas SP, Garris CS, Kohler RH, Kitaoka M, Cuccarese MF, Yang KS, et al. In vivo imaging reveals a tumor-associated macrophage – mediated resistance pathway in anti – PD-1 therapy. Sci Transl Med. 2017;1–10.

21. Marvel D, Gabrilovich DI. Myeloid-derived suppressor cells in the tumor microenvironment : expect the unexpected. J Clin Investig. 2015;125:3356–64.

22. Lavin Y, Kobayashi S, Leader A, Amir E ad D, Elefant N, Bigenwald C, et al. Innate Immune Landscape in Early Lung Adenocarcinoma by Paired Single-Cell Analyses. Cell [Internet]. Elsevier Inc.; 2017;169:750–765.e17.

23. Korehisa S, Oki E, Iimori M, Nakaji Y, Shimokawa M, Saeki H, et al. Clinical significance of programmed cell death-ligand 1 expression and the immune microenvironment at the invasive front of colorectal cancers with high microsatellite instability. Int J Cancer. 2018;142:822–32.

24. Adams A, Vail P, Ruiz A, Mollaee M, McCue P, Knudsen E, et al. Composite analysis of immunological and metabolic markers defines novel subtypes of triple negative breast cancer. Mod Pathol. 2018;2:288–98.

25. Harada K, Dong X, Estrella JS, Correa AM, Xu Y, Hofstetter WL, et al. Tumor-associated macrophage infiltration is highly associated with PD-L1 expression in gastric adenocarcinoma. Gastric Cancer. Springer Japan; 2018;21:31–40.

26. Heeren AM, Punt S, Bleeker MC, Gaarenstroom KN, Van Der Velden J, Kenter GG, et al.

Prognostic effect of different PD-L1 expression patterns in squamous cell carcinoma and adenocarcinoma of the cervix. Mod Pathol [Internet]. Nature Publishing Group; 2016;29:753–63.

27. Kubota K, Moriyama M, Furukawa S, Rafiul HASM, Maruse Y, Jinno T, et al. CD163+CD204+ tumor-associated macrophages contribute to T cell regulation via interleukin-10 and PD-L1 production in oral squamous cell carcinoma. Sci Rep [Internet]. Springer US; 2017;7:1–12.

28. Morrell ED, Wiedeman A, Long SA, Gharib SA, West TE, Skerrett SJ, et al. Cytometry TOF identifies alveolar macrophage subtypes in acute respiratory distress syndrome. JCI Insight [Internet]. 2018;3:1–11.

29. Roghanian A, Stopforth RJ, Dahal LN, Cragg MS. New revelations from an old receptor: Immunoregulatory functions of the inhibitory Fc gamma receptor, FcγRIIB (CD32B). J Leukoc Biol. 2018;1–12.

30. Madorsky Rowdo FP, Baron A, Urrutia M, Mordoh J. Immunotherapy in cancer: A combat between tumors and the immune system; you win some, you lose some. Front Immunol. 2015;6:2–13.

31. Du S, McCall N, Park K, Guan Q, Fontina P, Ertel A, et al. Blockade of Tumor-Expressed PD-1 promotes lung cancer growth. Oncoimmunology. 2018;

FIGURE LEGENDS

Figure 1. Immunohistochemical analyses for CD163, PD-L1 and CD33 in representative hyperprogressor and non-hyperprogressor cases.

(A) Representative microphotographs detailing the presence of macrophages displaying epithelioid morphology and expression of CD163, PD-L1, and CD33 markers (defined as *complete phenotype*) in four hyperprogressor cases. **(B)** Double immunofluorescence staining for CD163 (green) and PD-L1 (red) showing the co-expression of the two markers in epithelioid macrophages (arrows). **(C)** Representative microphotographs detailing the presence of macrophages displaying epithelioid morphology, variable clustering and the incomplete expression of the three CD163, PD-L1, and CD33 markers (defining the complete phenotype of HP patients) in two cases of non-HP patients (stable disease). **(D)** Representative microphotographs detailing the presence of myeloid elements with non-epithelioid morphology (stellate or spindle-shaped cells) on CD163, PD-L1, and CD33 markers populating tumor infiltrates of non-HP patients (one stable disease and one response). (**E**) Representative microphotographs relative to Arginase-A1 expression by clustered epithelioid macrophages in four HP patients' infiltrates. Magnification 20x.

Figure 2. CD33, CD163, and PD-L1 co-localization in clustered macrophages with epithelioid morphology

Immunofluorescence panels from prototypical hyperprogressive disease infiltrates showing the co-localization of CD33, CD163, and PD-L1 in clustered macrophages with epithelioid morphology. Three different combinations of double-marker stainings are shown. Green signal and red signal correspond to Opal-520 and Opal-620 fluorophores, respectively. Original magnifications x100 and x400.

Figure 3. Anti Mouse PD-1 Antibody Induces Tumor Progression in Athymic Mice

Athymic nude mice were xenografted with H460 lung cancer cell lines and treated i.p. (n=6 mice/group) (**A**) or p.t. (n=5 mice/group) (**B**) with 200µg of anti-mouse PD-1 blocking antibody (red dots) or with vehicle (black dots). Red arrows indicate the days of anti-PD-1 antibody

553 treatment. Dots represent Mean ± SEM of tumor volume for each group. **P <0.01 by Mixed
554 Models ANOVA. (**C**) Representative immunohistochemistry images and quantification of
555 leukocytes ($CD45^+$), macrophages ($F4/80^+$), Arginase-I^+, B lymphocytes ($CD45R/B220^+$),
556 granulocytes ($Gr\text{-}1^+$) and NK ($NKp46^+$) cells in the tumor microenvironment of H460 lung cancer
557 xenografts collected from the study illustrated in Figure 2B (p.t. experiment, n=5 mice/group).
558 Original magnification x20. *P <0.05, **P <0.01 by Mann-Whitney U test. (**D**) Athymic nude mice
559 were xenografted with H460 lung cancer cell lines and treated i.p. with 200 µg anti-PD-1 $F(ab)_2$
560 (blue dots) or with vehicle (black dots) (n=6 mice/group). Blue arrows indicate the days of anti-PD-
561 1 antibody treatment. Dots represent Mean ± SEM of tumor volume for each group.

562 **Figure 4. Anti Human PD-1 Antibody (Nivolumab) Induces Tumor Progression of PDXs in**
563 **SCID Mice**

564 (A) PDX302 (P53C135Y, EGFRL858R, KRASWT, APCWT) and PDX305 (P53WT, EGFRWT,
565 KRASG13C, APCR1114L) samples were injected in both flanks of SCID mice (n = 4). Mice were
566 treated with 10 mg/kg i.p. Nivolumab (red dots) twice weekly from day 1 after tumor implant to the
567 end of the experiment. **P < 0.01 by mixed models ANOVA. (B) Analysis of tumor cells
568 disseminated to mice lungs. Mice lungs were analyzed by FACS, after tissue dissociation to single
569 cells, for the presence of human disseminated cells. Graphs indicate the percentage of human cells
570 in Nivolumab treated and control mouse lungs. *P < 0.05 (C) Representative images showing
571 F4/80+ cells with epithelioid/monocytoid elements aggregated in clusters in an untreated PDX302
572 model. (D) Dot plot summarizing the results of the effects of Nivolumab treatment in all tested
573 PDX (PDX302, PDX305, PDX111, and PDX220) and xenograft models (H460 and PC9).
574 Response rate was estimated as described in the Materials and Methods section. (E) PDX302
575 (P53C135Y, EGFRL858R, KRASWT, APCWT) samples were injected in both flanks of SCID
576 mice (n = 4). Mice were treated with 10 mg/kg i.p. Nivolumab, Nivolumab F(ab)2 or clodronate
577 plus Nivolumab twice weekly (once weekly for clodronate injection) from day 1 after tumor
578 implant to the end of the experiment. *P < 0.05. (F) Analysis of tumor cells disseminated to mice

lungs. Mice lungs were analyzed by FACS, after tissue dissociation to single cells, for the presence of human disseminated cells. Graphs indicates the percentage of human cells in Nivolumab-, Nivolumab $F(ab)_2$- or Clodronate plus Nivolumab treated and control mouse lungs. *$P < 0.05$ compared to control; $^{\#}P < 0.05$ compared to Nivolumab-treated (G) Representative IHC images of mouse iliac lymph nodes show tumor cell dissemination with the presence of a metastatic nodule (indicated by the asterisk) only in Nivolumab-treated mice (H/E: hematoxylin/eosin staining; CK: pan-cytokeratin staining). (H) H&E and Masson's trichrome staining showing the presence of fibrotic areas with consistent matrix deposition in Untreated, Nivolumab- and Nivolumab $F(ab)_2$-treated representative cases. IHC analysis for $CD206^+$ macrophages highlighting the enrichment in macrophages in Nivolumab treated tumor.

Figure 5. Hypothesized mechanism through which macrophages and ICI are involved in determining HP

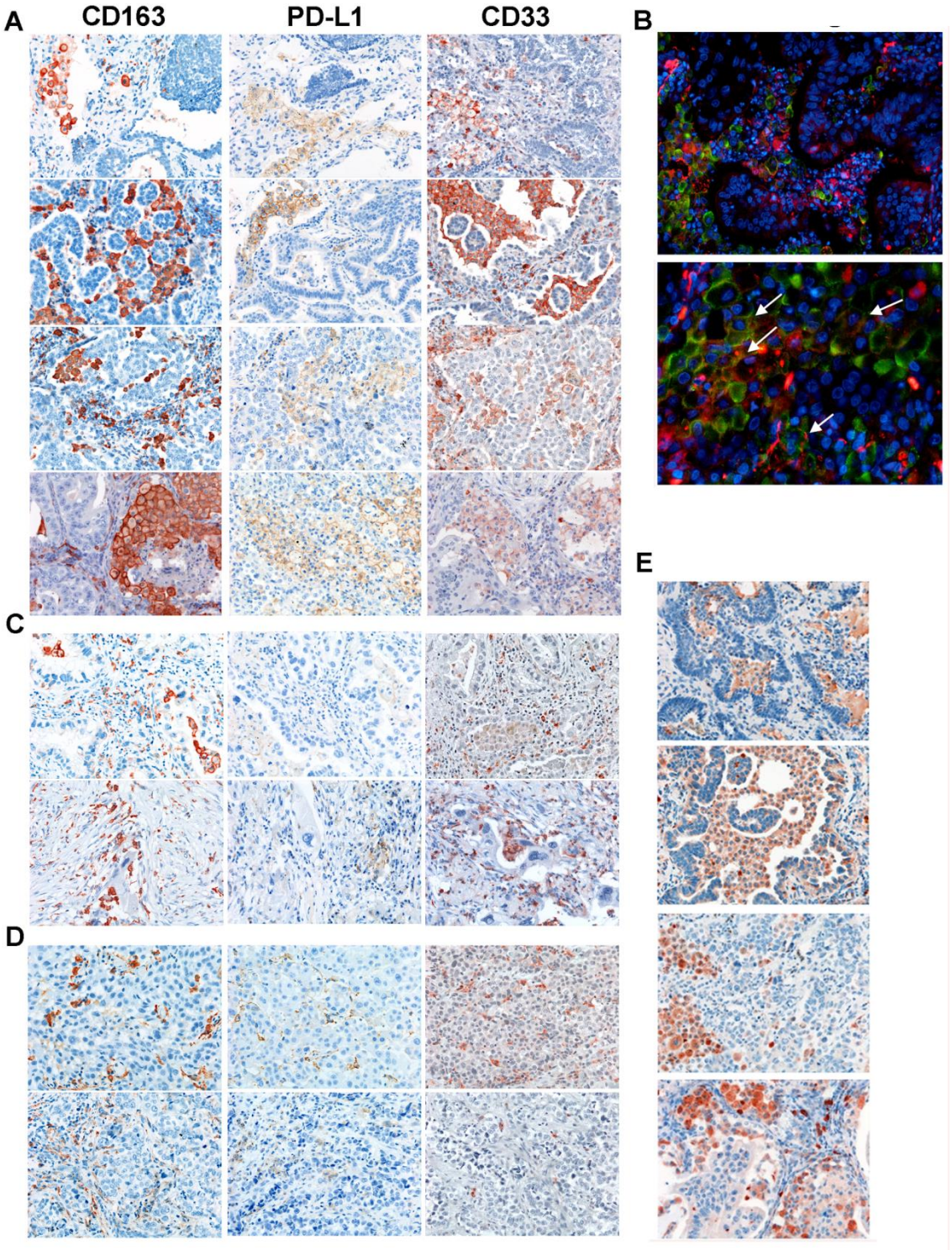

Figure1

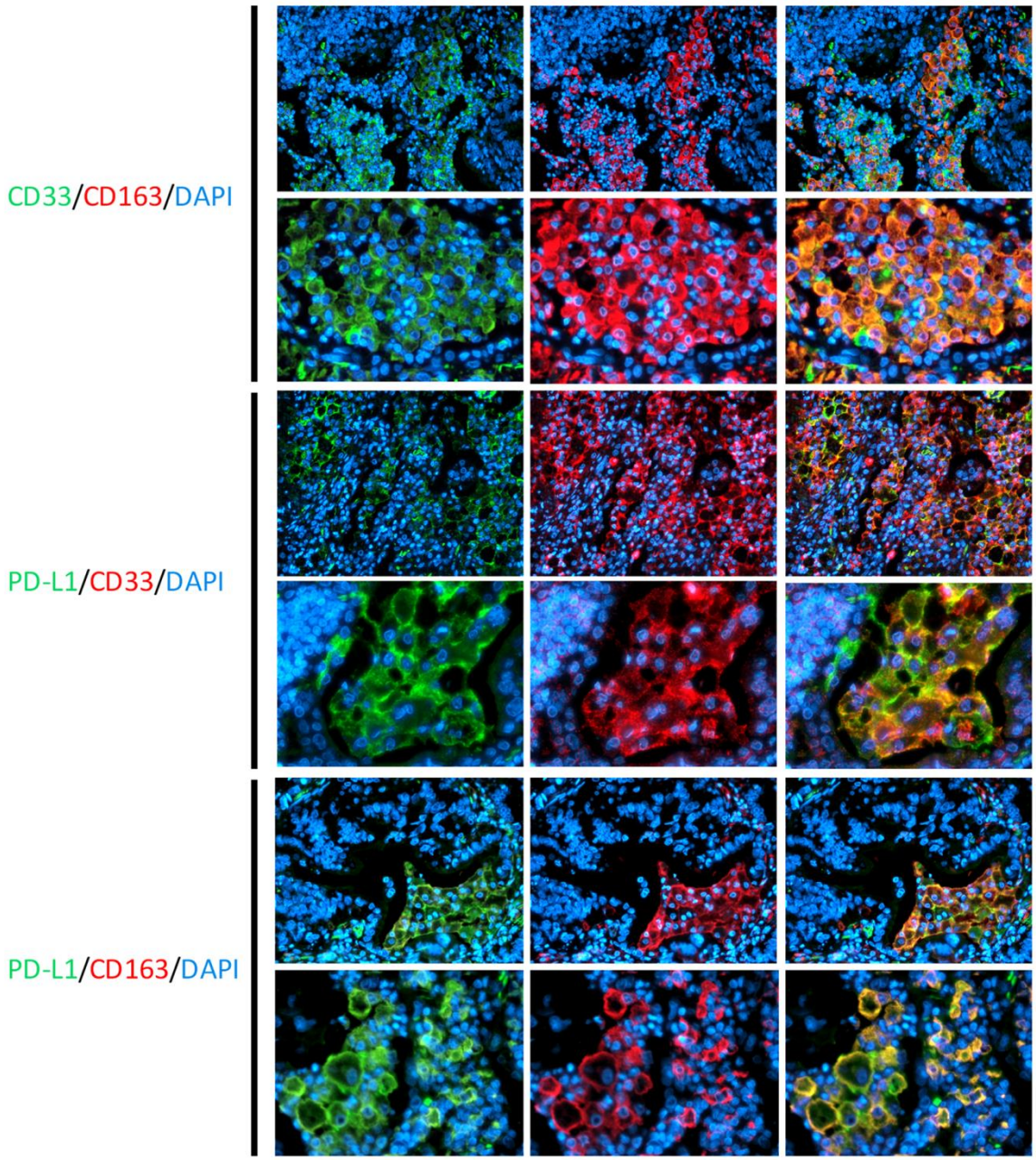

Figure2

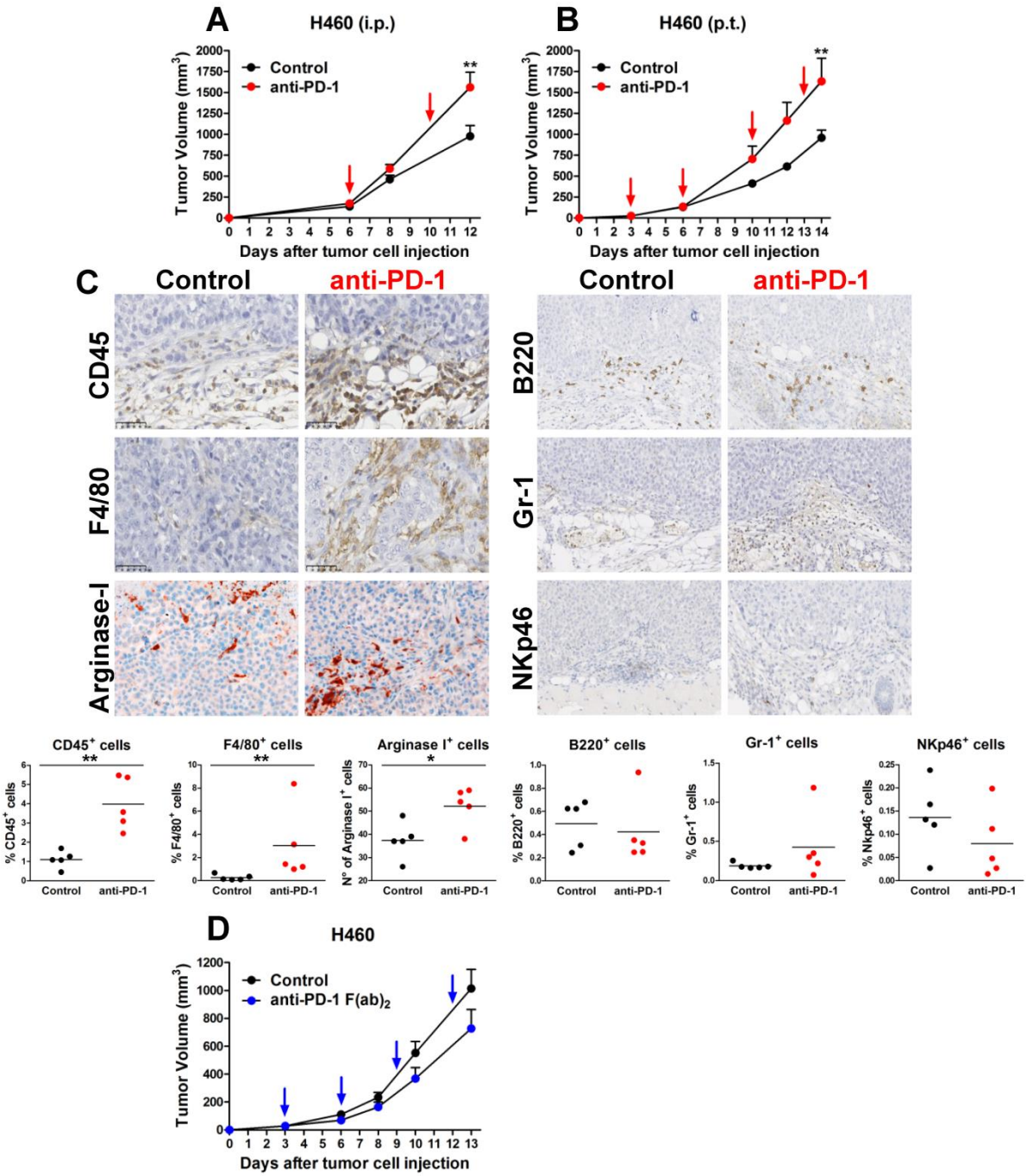

Figure3

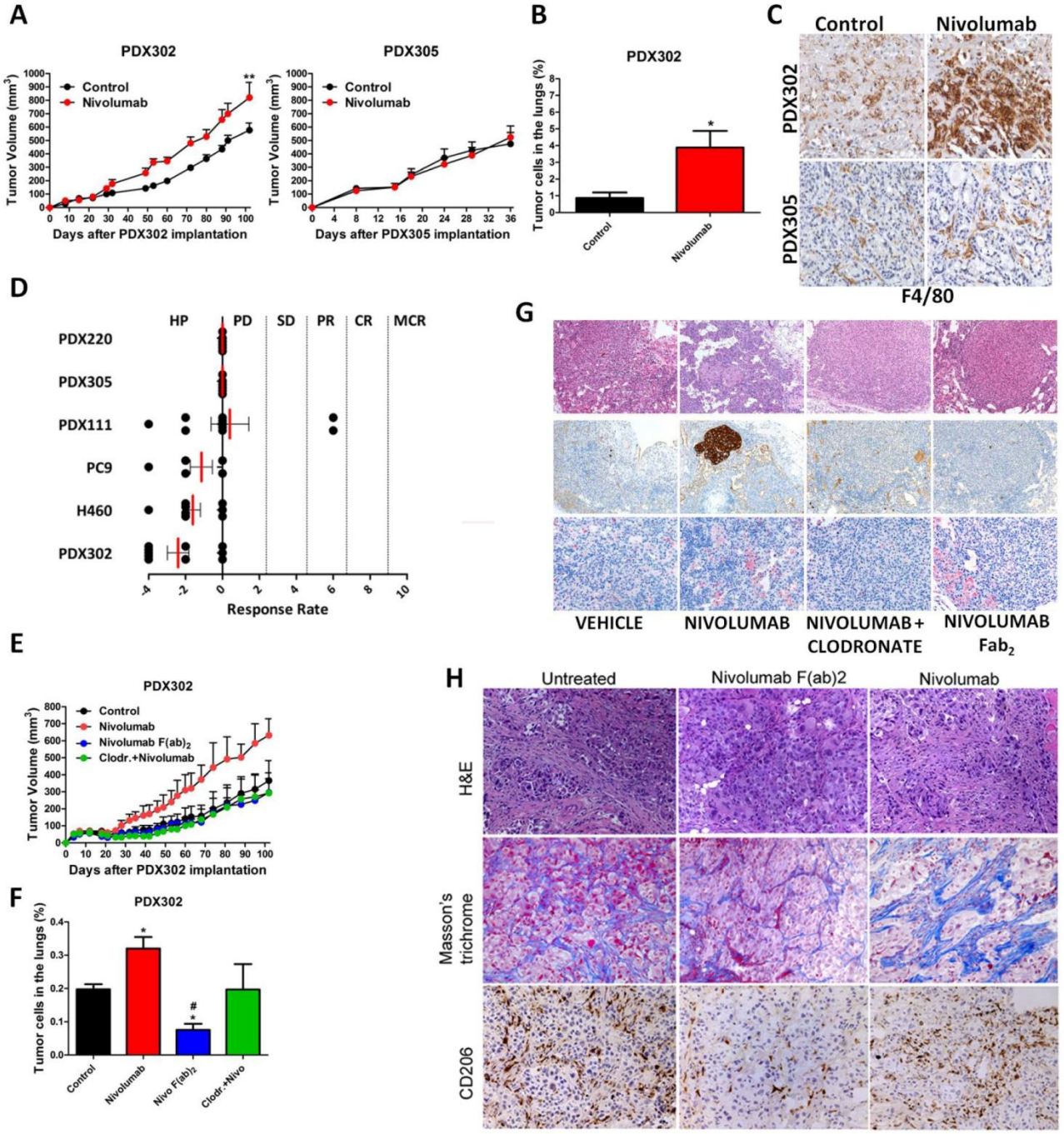

Figure 4

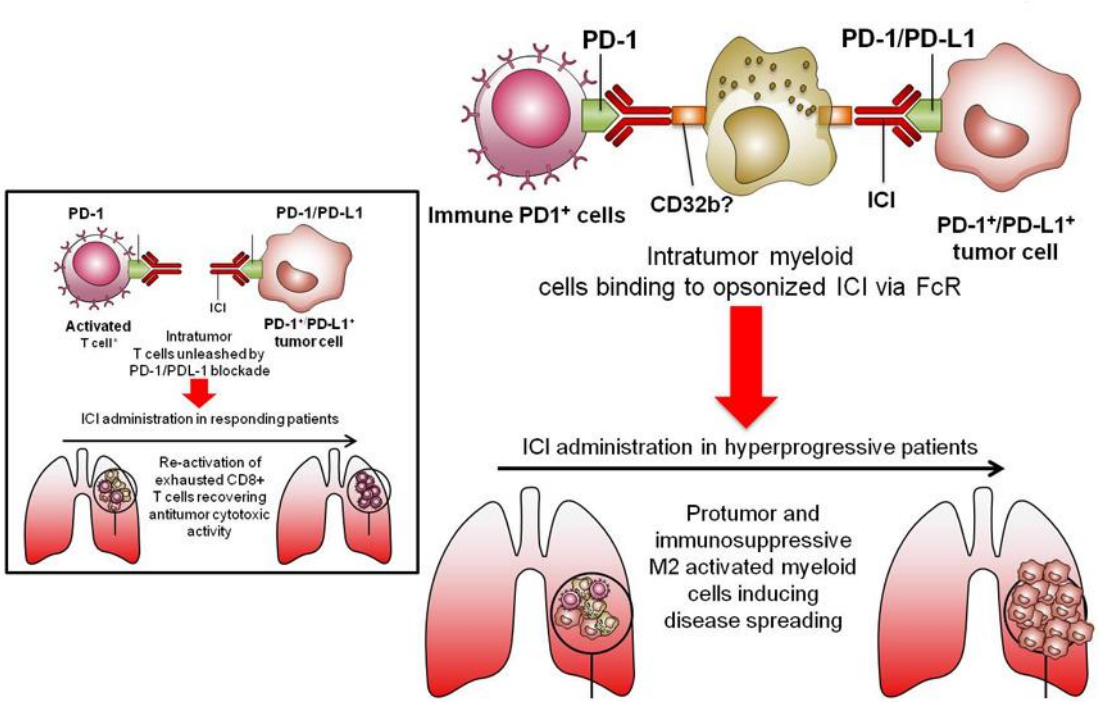

Figure5

AACR American Association for Cancer Research

Clinical Cancer Research

Antibody-Fc/FcR Interaction on Macrophages as a Mechanism for Hyperprogressive Disease in Non-Small Cell Lung Cancer Subsequent to PD-1/PD-L1 Blockade

Giuseppe Lo Russo, Massimo Moro, Michele Sommariva, et al.

Clin Cancer Res Published OnlineFirst September 11, 2018.